Awareness Messages by Vulnerable Road Users and Vehicles: Field Tests via LTE-V2X

Luca Lusvarghi, *Graduate Student Member, IEEE*, Carlo Augusto Grazia, *Member, IEEE*, Martin Klapez, *Member, IEEE*, Maurizio Casoni, *Senior Member, IEEE* and Maria Luisa Merani, *Senior Member, IEEE*

***Abstract*—Awareness messages have been recently introduced to extend the information horizon of connected vehicles and Vulnerable Road Users (VRUs) beyond their line-of-sight range. As of today, only a handful of studies has experimentally analyzed the awareness messages generated by cars, and no existing work has concentrated on VRU awareness messages. The intent of this work is to fill the gap of missing experimental activities by analyzing the results of an extensive measurement campaign, aimed at investigating the awareness messages generated by cars and VRUs in a real-world context. Field tests have been performed employing an LTE-V2X prototype with connected VRUs in the urban scenario, while cars have been considered in urban, suburban, and highway environments. In all cases, the paper details the conditions that trigger the generation of awareness messages, presents the Probability Mass Function (PMF) of the time interval between consecutive messages, and relates it to the triggering conditions. As the findings indicate that many awareness messages from VRUs were generated under non-relevant circumstances, the paper also proposes an adjustment to the standard and evaluates its effectiveness in the field, showing a notable improvement with respect to the original setting. Finally, this study evaluates the Packet Delivery Ratio (PDR) experienced by vehicle-to-vehicle communications in the above scenarios and, for the first time, determines the PDR attained by bicycle-to-vehicle communications in the urban setting.**

***Index Terms*—Vulnerable Road Users, VRU, VAM, CAM, road safety, LTE-V2X, V2V.**

I. Introduction

A variety of users travel on modern roads, experiencing heterogeneous safety levels. Occupants of vehicles move in a protected manner, while pedestrians, bikers, and, more generally, VRUs are more exposed to road accidents. Although the most advanced societies witness an increased sensitivity to sustainable mobility and healthy lifestyles, thus encouraging walking and cycling, the efficacy of the solutions to protect VRUs has not proceeded with the same impetus.

Wireless communications play a fundamental role in turning roads into safer traveling environments. As of today, the interest gravitates around vehicular communications that rely on competing and incompatible standards, i.e., the long-established IEEE 802.11p [1] [2], whose European counterpart is the Intelligent Transport System-G5 (ITS-G5) [3], rivals with the cellular-based approach, LTE-Vehicle-to-Everything (LTE-V2X) [4]. The advantages and drawbacks of the two technologies have been studied by several works over the last years, e.g., see [5]–[7], and new coexistence mechanisms have also been put forth [8].

Recently, special messages have been formalized at the application layer by both the Society of Automotive Engineers (SAE) and the European Telecommunications Standards Institute (ETSI), to support Day-1 safety services [9] [10]. VRUs and vehicles will broadcast them to make neighbors aware of their position, dynamics, and relevant attributes. Adhering to ETSI terminology, such awareness messages are distinguished in Cooperative Awareness Messages (CAMs) and VRU Awareness Messages (VAMs): the former are disseminated by cars and motorbikes, the latter by VRUs. Regarding VRUs, the white paper [11] published by the 5G Automotive Association (5GAA) emphasized the arising concern and the priority that 5GAA is giving to VRUs protection. In the first half of 2021, the document [12] also drew a general panorama and highlighted how roadside infrastructures could enhance the vehicles' awareness of VRUs.

As of today, the generation of CAMs has been mainly investigated through simulations and only few papers have experimentally analyzed the awareness messages generated by cars. Moreover, no existing work has concentrated on VAM dissemination. Hence, the intent of this work is to fill the gap of missing experimental activities by presenting the findings of a measurement campaign conducted to provide a broad view of the messages generated by VRUs, i.e., bicycles, e-scooters, and motorbikes, as well as by cars. The underlying assumption is that they are all connected and, therefore, able to transmit and receive. Commercially available LTE-V2X modules for direct communications, requiring no support from the cellular infrastructure, were employed. The ETSI algorithms formalized in [9] and [10] were implemented in the firmware of the boards, to broadcast VAMs and CAMs with the proper timing.

First, VRUs in an urban environment were considered: the Probability Mass Function (PMF) of the time between the generation of consecutive VAMs was experimentally determined, and the various causes that triggered the transmission of such messages were identified for bicycles and e-scooters. The investigation was performed employing the VAM generation rules recommended by ETSI in [10]. The analysis revealed that many VAMs were unnecessarily generated; this urged for the proposal of an alternative. The intent was to

The authors are with the Department of Engineering "Enzo Ferrari", University of Modena and Reggio Emilia, Modena 41125, Italy (e-mail: luca.lusvarghi5@unimore.it, carloaugusto.grazia@unimore.it, martin.klapez@unimore.it, maurizio.casoni@unimore.it, and marialuisa.merani@unimore.it) and also with Consorzio Nazionale Interuniversitario per le Telecomunicazioni, CNIT. Contact author: Maria Luisa Merani. This work was partly funded by a 2022 FAR grant of Dipartimento di Ingegneria "Enzo Ferrari".

Manuscript received XXX, XX, 2015; revised XXX, XX, 2015.

avoid generating too many VAMs, that excessively clutter the radio channel, without missing relevant information about the VRU movements. The same characterization was attained for motorbikes by employing CAMs, determining the temporal features of the messages broadcasted by this category of road users.

Next, field tests were performed for cars traveling in urban, suburban, and highway scenarios, where the generation times of CAMs were critically analyzed. Lastly, the Packet Delivery Ratio (PDR) attained by the LTE-V2X technology in Vehicle-to-Vehicle (V2V) and, for the first time in the literature, bicycle-to-vehicle communications was experimentally determined.

The most relevant contributions this work provides can be summarized as follows:

- for the first time in the literature, awareness messages generated by VRUs were analyzed in an urban environment, highlighting their peculiarities;
- an adjustment to reduce the unnecessarily high generation rate of VAMs was proposed and proved successful;
- the PDR of VAMs received by a car through bicycle-to-vehicle communications was evaluated in the urban scenario;
- for CAMs, the different causes of vehicles' message generation were disclosed in the urban, suburban, and highway environments;
- the PDR of CAMs received by cars through direct vehicle-to-vehicle communications was evaluated in the above scenarios, revealing more pessimistic results than in controlled field tests.
- the entire dataset of experimental results was made publicly available [13].

The rest of the paper is organized as follows. Section II positions the current work in literature. Section III introduces the VRU definition and illustrates the rules to follow when VRUs generate awareness messages. The commonalities and differences from CAMs are also highlighted. Section IV details the measurement campaign that broadcasted and collected VAMs and CAMs, and critically analyzes the data provided by the field tests. Section V draws the conclusions.

II. Related Work

As a matter of fact, the broadcasting of awareness messages by VRUs has never been the subject of field tests, nor has a unified analysis of CAM delivery in different environments been put forth with reference to the LTE-V2X technology. To corroborate the above statement, this Section offers a panorama on some among the most relevant studies in the field and strives to evidence the novel contribution of the current work.

A few papers that recently focused on VRUs are [14]-[19]. In exploring this research area, the majority of these studies took a simulative approach, which the present work well complements. At application layer, [14] and [15] dealt with the motion prediction of VRUs, focusing on artificial intelligence techniques to predict trajectories and detect VRUs. The authors of [16] further demonstrated that VAM adoption enables the early triggering of the Forward Collision Warning (FCW) system; as the focus was on the FCW improvement, the details and dynamics of VAM generation were neglected. More recently, [17] investigated how the combination of VAMs and cooperative perception messages increases the VRU detection rate in a simulated roundabout scenario. Novel solutions to increase the awareness of vehicles with respect to VRUs were experimentally explored in [18] and [19]. The former study examined vehicles equipped with 802.11p-based devices, communicating with intelligent roadside units. The latter document targeted different 5G enabled use cases, among which the protection of VRUs. Both works took the vehicle perspective and ignored the possibility that VRUs broadcast awareness messages. Furthermore, these studies relied on an infrastructured approach, whereas our contribution is centered on direct communications among VRUs and vehicles.

Among CAM studies, [20] explored the practical limits of cooperative awareness in vehicular communications. Relying upon field tests, this work computed the PDR attained by CAM dissemination employing ITS-G5 devices. More recently, [21] and [22] performed an experimental comparison between ITS-G5 and LTE-V2X, but the assessment was performed in a controlled environment [21] or confined to highway communications [22]. Moreover, in [20] and [22] CAMs were periodically issued, which is not what the ETSI standard dictates [9], whereas the authors of [21] did not consider CAM traffic. The study published in [23] highlighted the diverse nature of the CAM messages of two different car manufacturers, in size and transmit rate. Unlike the current investigation, [23] did not explore the causes behind CAM generation or made the collected traces publicly available. Furthermore, the data collection was very modest, limited to a few tens of minutes. A paper on benchmark testing of the V2X technology is [24], which however discussed an analysis performed in a well controlled context, i.e., a field track. A controlled environment has also been leveraged by the authors of [25], who employed an indoor testbed to experimentally assess the robustness of the LTE-V2X technology against denial-of-service attacks. On the contrary, the present work intends to experiment with LTE-V2X in a real setting and to put this technology at the service of VRUs.

In the authors' previous investigations, the coexistence of aperiodic, CAM-like traffic, with periodic flows in LTE-V2X was studied [26]. In [27], a machine-learning based enhancement to the LTE-V2X standard was proposed, to predict when CAMs are generated and how to effectively reserve radio resources for their transmissions. The present work undertakes an experimental approach for the transmission of awareness messages via LTE-V2X. The investigation zooms into the generation process of VAMs and CAMs, and dissects their causes, demonstrating that they largely vary, depending on the type of road users and the examined scenario. Furthermore, the work evaluates the PDR performance of LTE-V2X when employed for direct communications between a bicycle transmitting VAMs and a car in the urban setting, as well as its performance when broadcasting CAMs via direct V2V communications in urban, suburban, and highway settings. Finally, the paper makes available to the scientific community

the entire dataset collected during the field tests; unlike car manufacturers, which reluctantly provide their measurements and only disclose their final outcomes, we offer the scientific community both.

III. Vulnerable Road Users

A. VRU definition, features, and requirements

Although the most diffused road occupants are vehicles, a growing interest is currently being reserved for those road users that either do not use a mechanical device for their trips or utilize alternative means of transportation, less invasive than cars. Such "road inhabitants" are classified as VRUs by the ETSI standard document [28], which the current subsection mostly draws from. The following categories are identified:

- pedestrians;
- road workers;
- wheelchair users and prams;
- skaters;
- e-scooter riders;
- cyclists;
- scooter drivers;
- motorcycle drivers;
- animals such as dogs, horses, and wild animals which present a safety risk to other road users.

In [28], VRUs are further categorized in three groups, each with its traits: VRU profile 1 mainly refers to pedestrians, whose behavior is often unpredictable and whose speed range is limited; VRU profile 2 includes light vehicles, that may be equipped with an electric engine: they move at a relatively low speed and their behavior can be more easily predicted than for pedestrians, yet it is still subject to random movements; VRU profile 3 includes motorbikes, whose speed is similar to cars and that exactly like vehicles can send CAMs when properly equipped. Every profile exhibits its own challenges: VRUs belonging to profiles 2 and 3 are often hard to perceive from other vehicles; moreover, profiles 1 and 2 VRUs sometimes travel in groups and do not follow road rules.

In the upcoming years, VRU safety will go through the widespread adoption of wireless connectivity: when connected, the VRU can either have only a transmitter that broadcasts awareness messages or a receiver for messages from other road users and roadside units, or both.

The transmission of VRU standard messages, the so-called VAMs, is needed in the majority of cases. To reduce the amount of load that VAMs would generate on the radio channel at specific occurrences, for instance, at a pedestrian crossing in a metropolitan area or at a location where a major event takes place, VRUs are grouped in a new logical entity, termed cluster [29]. Users belonging to the same cluster may belong to the same profile or exhibit different profiles; however, they move with similar speed or direction and within a bounding box. Importantly, other road users are informed of the cluster presence through a single VAM, rather than by a VAM for each VRU. It is up to the cluster head to issue the VAM and indicate whether the cluster is homogeneous or heterogeneous; the latter difference is particularly useful, as it offers information about the trajectory and behavior prediction once the cluster disperses.

TABLE I
Adopted Symbols.

Symbol	Definition
T_{VAM}	Time interval between consecutive VAMs
T_{GenVam}	Minimum time interval between consecutive VAMs (it depends on the congestion control algorithm employed)
$T_{GenVamMin}$	T_{GenVam} lower bound (recommended value: 100 ms)
$T_{GenVamMax}$	T_{GenVam} upper bound (recommended value: 5000 ms)
$T_{CheckVamGen}$	Periodicity at which VAM triggering conditions are checked
T_{CAM}	Time interval between consecutive CAMs
$T_{GenCamMax}$	Maximum allowed time between consecutive CAMs (1000 ms)

B. VRU Awareness Messages

The current Section explains the generation rules and format of VAMs. It then shortly elaborates on CAMs, which are much more frequently encountered in literature than VAMs, citing the related works. The adopted symbols are reported in Table I.

1) VAM generation: The ETSI standard document [10] dictates that the minimum time elapsed between consecutive VAM generation events has to be equal to or larger than T_{GenVam}, where T_{GenVam} falls in the interval $[T_{GenVamMin}, T_{GenVamMax}] = [100, 5000]$ ms. Furthermore, an individual VAM is generated whenever:

(i) the time elapsed since the last VAM transmission exceeds $T_{GenVamMax}$;
(ii) the absolute distance between the current VRU position and the one included in the previous VAM exceeds $\Delta_d = 4$ m;
(iii) the absolute difference between the current VRU heading and the heading included in the previous VAM exceeds $\Delta_h = 4°$;
(iv) the absolute difference between the VRU current speed and the speed included in the previous VAM exceeds $\Delta_s = 0.5$ m/s;
(v) the difference between the currently estimated trajectory interception probability with vehicles(s) or other VRU(s) and the trajectory interception probability with vehicle(s) or other VRU(s) lastly reported in a VAM exceeds a threshold;
(vi) the VRU decides to join a cluster;
(vii) the VRU has determined that one or more new vehicles or other VRUs are coming closer than the minimum safe lateral distance or the minimum safe longitudinal distance or the minimum safe vertical distance.

The conditions for triggering the VAM generation shall be checked every $T_{CheckVamGen}$, where $T_{CheckVamGen} \leq T_{GenVamMin}$ [10].

If the VRU is exclusively equipped with a transmitter, conditions (v) and (vii) do not apply. Last, condition (vi) comes into play when a cluster of VRUs is considered. Finally, redundancy mitigation techniques are enforced to reduce the

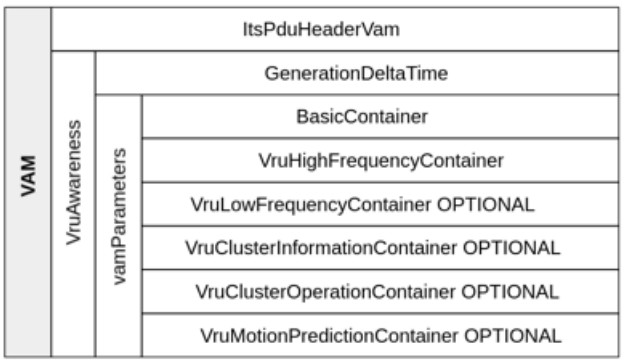

Fig. 1. VAM structure.

communication load in settings where VRUs can be very numerous without compromising safety or awareness. Here, the underlying ideas are: (i) to decrease VAM frequency by a given factor when a peer system (e.g., another VRU) has just issued a VAM while being in very similar conditions as the reference VRU in terms of location, speed, and orientation; (ii) to skip VAM transmission in a non-drivable or low-risk geographical area.

2) VAM format: The VAM format includes the ITS Protocol Data Unit (PDU) header, generation time, and multiple data containers, as illustrated in Fig. 1. The ITS PDU header adheres to a common format that is employed for application and facility layer messages: it contains data elements such as the identifier of the transmitting VRU and the message ID. The message ID indicates the message type, and it is set to 14 for VAMs.

After the header and the timestamp, the Basic Container and the High-Frequency Container represent the first two components of the payload. According to the standard, these are mandatory containers that shall be included in every transmitted VAM. In detail, the Basic Container provides fundamental information about the VRU generating the awareness message, such as the VRU type (e.g., pedestrian, cyclist) and its latest geographical position. Next to the Basic Container, the High-Frequency Container has been designed to provide fast-changing information, such as the latest heading, speed, and acceleration values that the originating VRU has retrieved. Moreover, this container may include optional information used only by specific VRU profiles. In addition to the mandatory containers, a VAM shall also include the Low-Frequency Container when the time elapsed since the last VAM transmission exceeds 2000 ms. As opposed to the High-Frequency Container, the Low-Frequency Container holds slow-changing information, like the VRU profile and size. In this case, too, the container's content comprises both mandatory and optional data elements.

With reference to CAMs, VAMs may include three additional containers: the Cluster Information Container, the Cluster Operation Container, and the Motion Prediction Container. When two or more users operate within a cluster, the cluster leader shall include the Cluster Information Container in its transmitted VAMs. Specifically, this container is used to disseminate basic information about the VRU cluster, such as the cluster ID, the cluster bounding box, and the profiles of the VRUs forming the cluster. On the other hand, the Cluster Operation Container can be included by either the cluster leader or a cluster member. The cluster leader exploits this container to announce the cluster breakup and indicate the conditions that triggered such an event. Conversely, cluster members include the Cluster Operation Container in the transmitted VAMs when they perform cluster joining or leaving procedures. Last, the Motion Prediction Container is an optional payload component that provides information about the past and future movements of the originating VRU. This container can include up to 40 data entries that report the most recent activity of the VRU or predictions about its future trajectory.

As the VAM payload contains both mandatory and optional information, its size can significantly change depending on the considered VRU profile and the specific implementation. For instance, the size of the VRU Motion Prediction Container can vary from 45 to 1180 bytes depending on the number of data entries. The ETSI standard indicates that the VAM size lies between 40 and 1260 bytes if no or all optional containers are included, respectively. Furthermore, VAMs are tentatively harmonized with the Personal Safety Message (PSM) defined by SAE in [30].

Unlike VAMs, CAMs are often mentioned in scientific and technical literature, albeit the case of messages issued by motorbikes is never considered. The role of CAMs in enhancing road safety has been explored in various settings, e.g., see [31]–[33]. CAMs generation rules and format are given in the ETSI standard document [9] and appear in several papers [34], [35]. For a CAM, the message ID value that indicates the message type is 2. Moreover, with reference to Subsection III-B, the CAM generation times are ruled by the conditions (i)-(iv) previously listed, whereas conditions (v)-(vii) apply to VAMs only. Furthermore, $T_{GenCamMax}$ replaces $T_{GenVamMax}$, and $T_{GenCamMax} = 1$ s. It is worth pointing out that the Δ_d, Δ_h, and Δ_s thresholds are fixed in the case of CAMs, and can be adjusted when VAMs dissemination is considered. The CAM size ranges from 45 to 400 bytes, as highlighted in [36], and a further increase of some hundred bytes is due to the introduction of security content like signatures and certificates [23]. Overall, CAMs are less flexible in length and content than VAMs.

ETSI specifications do not indicate any recommended configuration regarding the number of size of the optional containers included in a CAM [9] (or VAM [10]). As a result, the format and the size of CAMs and VAMs depend on each specific implementation. Therefore, instead of tackling any arbitrary CAM or VAM implementation profile, this work concentrates on the message temporal patterns and considers a fixed message format that carries basic information, namely: the speed, the heading, and the spatial coordinates of the originating road user at the time of the message generation, and the sequence number of the generated message.

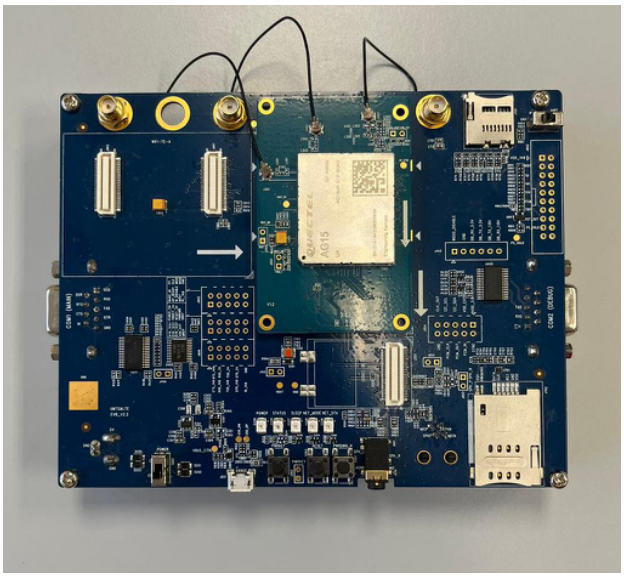

Fig. 2. Quectel evaluation board used for the field measurements.

IV. Field Tests

A. LTE-V2X boards

LTE-V2X was employed for the experimental tests. This technology was standardized by the Third Generation Partnership Project (3GPP) within Release 14 and recently paired with its 5G evolution, termed New Radio (NR)-V2X [37]. The LTE-V2X standard was ideated to support day-one safety applications, mainly based on the dissemination of CAMs, Decentralized Environmental Notification Messages (DENMs) [33], and Basic Safety Messages (BSMs). LTE-V2X envisions two distinct operating modes, termed Mode 3 and Mode 4. This study concentrates on Mode 4, where VRUs and vehicles autonomously select radio resources for their transmissions and directly communicate without cellular infrastructure support.

The experimental results were obtained employing the AG15 module, manufactured by Quectel [38]. The module embeds the Qualcomm 9150 C-V2X chipset, which is compliant with LTE-V2X Release 14 specifications and respects the quality constraints for automotive products set by the IATF 16949 standard. It supports Mode 4 vehicular communications in the n47 band ($5855 - 5925$ MHz). In accordance with the standard, every broadcasted VAM (and equivalently every CAM) is encapsulated in a Transport Block (TB) transmitted in the Physical Sidelink Shared Channel (PSSCH). The module also features a Global Navigation Satellite System (GNSS) multi-constellation receiver that allows for positioning, speed, and heading measurements. The constellations supported by the GNSS receiver are GPS, GLONASS, BeiDou, and Galileo. The module is mounted on the Quectel evaluation board shown in Fig. 2.

The board is equipped with 2 omnidirectional antennas, characterized by a 5 dBi gain. When installed on the rooftop of cars, the antennas were connected to the board using 50 Ω RG316 coaxial cables; when used on bicycles, they were directly inserted on the board, via Sub-Miniature Version (SMA) coaxial connectors. The transmit power and the receiver sensitivity were set to 23 dBm and -93 dBm, respectively. Because of the attenuation due to the coaxial cables and connectors, the emitted power was always lower than 28 dBm. Therefore, it fulfilled the requirement set by the EU regulation [39], which states that the maximum RF output power shall not exceed 33 dBm equivalent isotropically radiated power (e.i.r.p.) in the n47 frequency band. The adopted Modulation and Coding Scheme (MCS) index was 5, corresponding to 16 QAM modulation and to a $1/2$ code rate. This is a typical setting for LTE-V2X communications, also employed in simulative works [40], [41].

The algorithm that rules the generation of CAMs and VAMs was custom developed, adhering to the dissemination rules defined by ETSI in [9], [10]; in this respect, the availability of the high sensitivity GNSS receiver was fundamental to monitor the dynamics of the vehicle/VRU every 100 ms, and check whether one of the four position, heading, speed, and timeout conditions occurred (see conditions (i)-(iv) in Section III-B). Note that, as the input format of the GNSS data is fixed and the number of triggering conditions to be checked is also fixed, the computational complexity of the algorithm is constant and corresponds to $\mathcal{O}(c)$, where $c = 4$, as the number of conditions to check every 100 ms is 4. For the field tests, we have developed two different versions of the algorithm. The first version has been implemented as custom firmware in the Quectel AG15 boards for generating the messages in real-time. Compiling and running the algorithm on the boards required significant implementation efforts. The second version of the algorithm runs offline and can be employed to generate CAMs and VAMs from the playback of GNSS traces. This latter version of the algorithm can work with GNSS traces recorded by any device and has been instrumental to the investigation of different heading thresholds. The second version of the algorithm is available at [13].

As indicated at the end of Subsection III-B, both CAMs and VAMs employ a fixed message format that carries the essential pieces of information needed to trigger their generation. According to it, their size was constant and equal to 300 bytes.

B. Bicycle and E-scooter VAMs

In what follows, the VAM generation times of two different VRU types, a bicycle and an e-scooter, are analyzed. They were obtained by a VRU equipped with the Quectel board that recorded its GNSS output with a 10 Hz sampling frequency. Based on such output, the VAM traces were *a posteriori* generated, through custom Python scripts that allow for the setting of different threshold values in conditions (ii)-(iv).

TABLE II
Number of collected CAMs and VAMs.

Vehicle type	Urban	Suburban	Highway
Bicycle	44543	-	-
E-scooter	14437	-	-
Motorbike	40308	-	-
Car	18218	31222	16106

TABLE III
FIELD TEST REGION, DURATION, AND TRAVELED DISTANCE.

latitude in [44.575593,44.643645]	longitude in [10.859186,10.989253]		
Vehicle type	Urban	Suburban	Highway
Bicycle	3 hours, 42 km	-	-
E-scooter	2 hours, 26 km	-	-
Motorbike	4.5 hours, 128 km	-	-
Car	2 hours, 82 km	2 hours, 131 km	1 hour, 127 km

In accordance with the GNSS sampling period, the VAM triggering conditions of Subsection III-B were checked with a 10 Hz frequency, i.e., every $T_{CheckVamGen} = 100$ ms. Note that no receiving board is needed when measuring the time interval between consecutive CAMs and VAMs. We only need to monitor the dynamics of the vehicle/VRU that generates the messages. No other traffic participants broadcasting awareness messages were considered, so the case of a VRU-Tx only equipment, according to ETSI [28], was recreated. It followed that the VAM triggering conditions (v) and (vii) introduced in Subsection III-B1 could not be encountered. The VAM triggering condition (vi) could not be met either, as all the experiments involved a single VRU. Therefore, VAMs were caused either by a timeout event, i.e., by the occurrence of condition (i), or by events related to the VRU dynamics, i.e., by conditions (ii)-(iv).

The bicycle VAMs are analyzed first. They refer to an urban environment, namely, a residential suburb and the downtown area of the city of Modena, Italy. The rides took place in a propagation environment featuring no harsh urban canyons. For this setting, the dataset consists of 44543 VAMs, as reported in Table II. The duration of the experiments and the traveled distance are reported in Table III, which also details the latitude and longitude intervals of the area where all the tests took place.

Fig. 3 shows an exemplary portion of a bicycle VAM trace: T_{VAM}, the time between the generation of consecutive VAMs, is reported as a function of the VAM index. The trace was

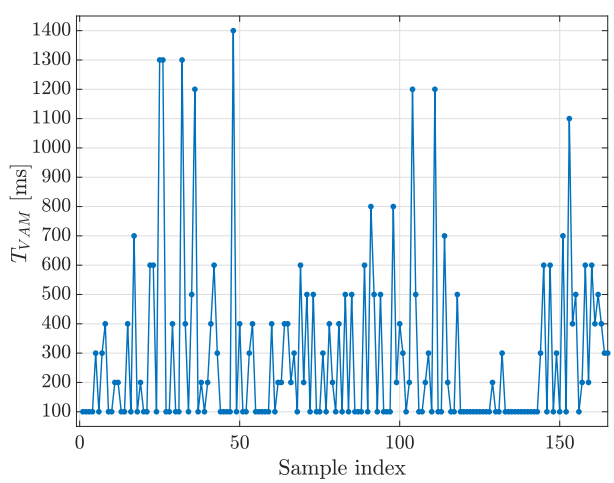

Fig. 3. Bicycle: VAM trace.

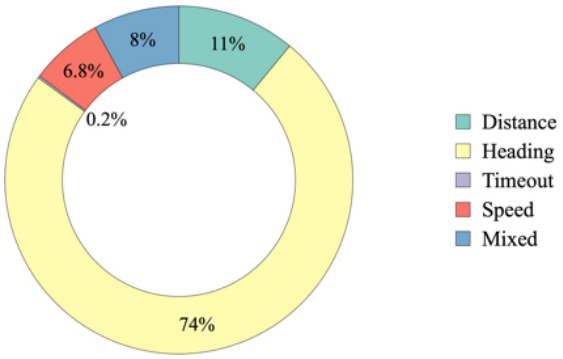

(a) Triggers distribution.

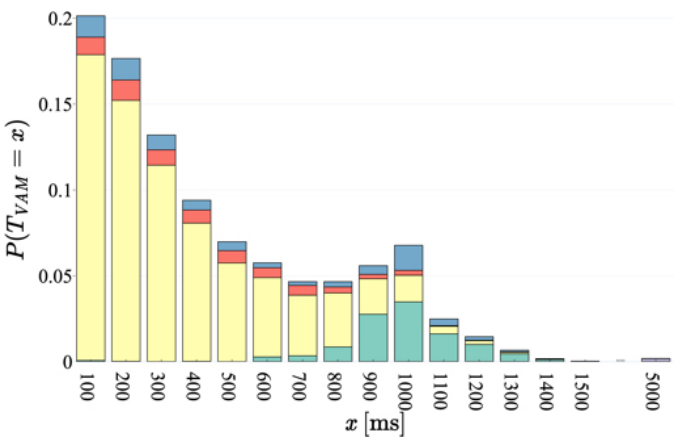

(b) PMF.

Fig. 4. Bicycle: VAM triggers and T_{VAM} PMF for $\Delta_h = 4°$.

obtained by setting the thresholds that trigger the VAM to $\Delta_d = 4$ m, $\Delta_h = 4°$, and $\Delta_s = 0.5$ m/s [10]. As expected, the minimum observed value of T_{VAM} is 100 ms, coinciding with $T_{CheckVamGen}$. The figure reveals that the VAM trace is fairly irregular: T_{VAM} rarely stays constant between consecutive samples unless specific conditions are met. An example of this is provided in the last portion of the trace, where the sample index falls in the $610 - 620$ interval, and T_{VAM} stabilizes at $700 - 800$ ms. Such behavior is typically observed when the bicycle follows a straight trajectory at an approximately constant speed.

Next, Fig. 4(a) reports the percentages of VAMs classified based on the triggering conditions (i)-(iv) at the end of Subsection III-B, for the same choice of thresholds as in Fig. 3. An additional type, labeled as "mixed", is considered; it indicates that a VAM was generated when more than one triggering condition was satisfied, an event not excluded by the standard. Interestingly, VAMs due to heading variations are the most frequent, accounting for 74% of the total. On the other hand, only 6.8%, 11%, 8%, and 0.2% of VAMs are generated by a speed, distance, mixed, and timeout trigger, respectively. The 98% of VAMs classified as "mixed" also satisfies the heading condition.

Fig. 4(b) completes the data analysis, displaying the PMF of T_{VAM}, the time between two consecutive VAMs. In this figure, the contributions to the PMF due to a variation in the VRU speed, heading, and distance, as well as to a timeout, are

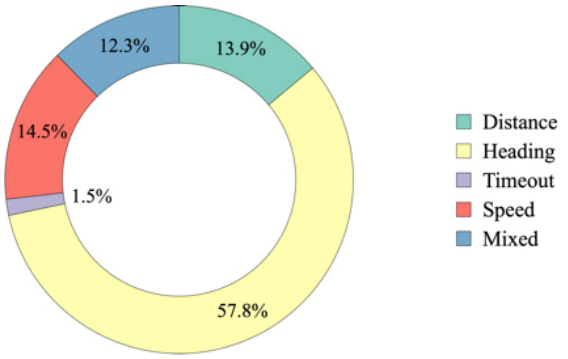

(a) Triggers distribution.

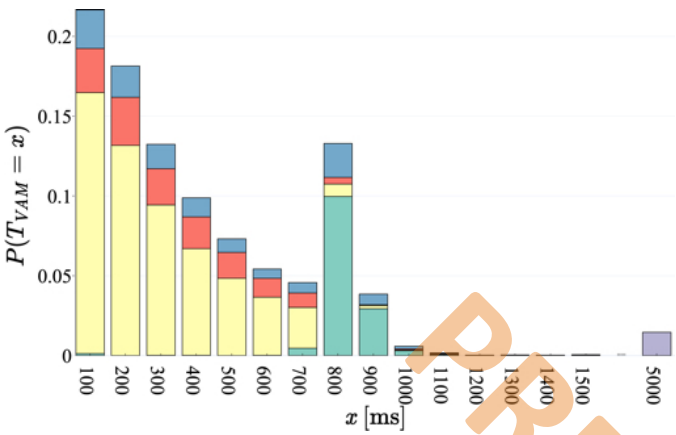

(b) PMF.

Fig. 5. E-scooter: VAM triggers and T_{VAM} PMF for $\Delta_h = 4°$.

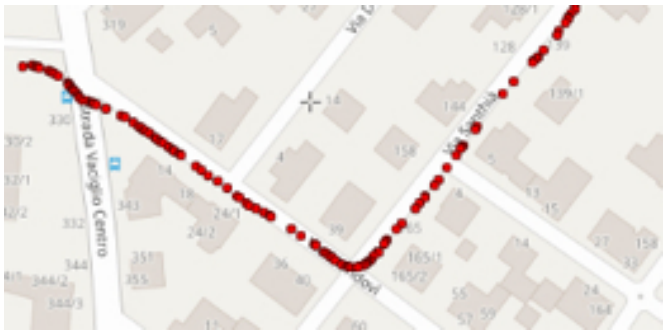

(a) $\Delta_h = 4°$.

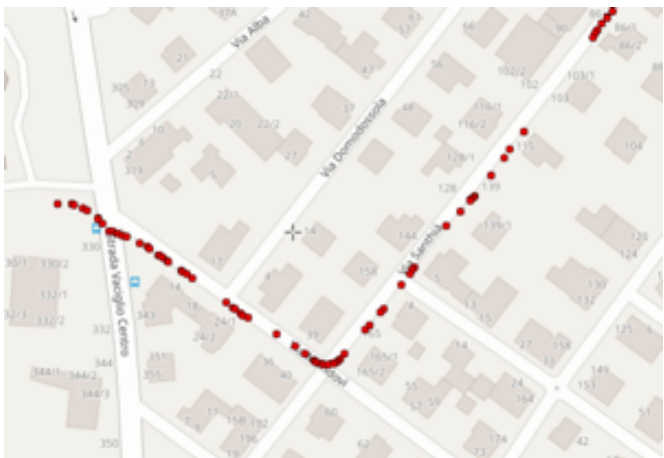

(b) $\Delta_h = 7°$.

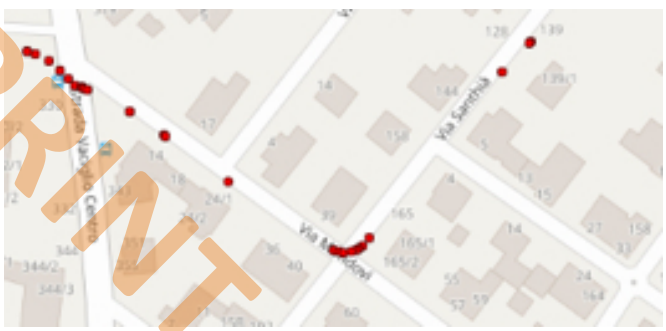

(c) $\Delta_h = 10°$.

Fig. 6. Bicycle: GNSS coordinates when heading-triggered VAMs are generated.

separately displayed. The figure reveals that VAMs triggered by heading variations greater than $\Delta_h = 4°$ are mainly observed for low T_{VAM} values. In constrast, VAMs due to distance variations greater than 4 m become predominant when T_{VAM} falls within the $800 - 1300$ ms range. The average and maximum bicycle speeds that were recorded are 12.9 and 27.7 km/h; under the assumption of uniform linear motion, the first value allows to conclude that it takes more than 1100 ms to cover a distance coincident with $\Delta_d = 4$ m. Fig. 4(b) also shows that the probability of observing T_{VAM} values in the $[1400, 5000]$ ms range is practically zero. $P[T_{VAM} = 5000 \text{ ms}]$ is insignificant too: this value is exclusively due to timeouts that occur if the bicycle stands still, as might be the case for a red traffic light. Such a situation was seldom encountered during an average bicycle ride, which explains the negligible fraction of VAMs generated by this condition.

The second type of VRU that was analyzed is the e-scooter. As for the bicycle, we begin our analysis considering the VAMs generated when $\Delta_d = 4$ m, $\Delta_h = 4°$, and $\Delta_s = 0.5$ m/s. The collected dataset led to 14437 VAMs and refers to routes leading to the downtown area of the city of Modena and to the city center. Fig. 5(a) shows that 57.8%, 13.9%, and 14.5% of the VAMs were generated by a heading, distance, and speed variation, respectively. This figure also indicates that mixed triggers represent 12.3% of the total and that the percentage of timeout triggers is negligible. The 94.7% of mixed triggers satisfies the heading condition. The PMF of T_{VAM} is reported in Fig. 5(b). As in Fig. 4(b), heading-triggered VAMs are mostly observed for small T_{VAM} values. Differently from the case of the bicycle, VAMs caused by distance variations are mostly concentrated at $T_{VAM} = 800$ and 900 ms, rather than being distributed over a wider range. This has probably to be ascribed to the speed-limited e-scooter employed for the tests, whose speed was more stable than that of the bicycle. In this setting, the recorded average speed was 14 km/h; the maximum was 25.1 km/h. Both figures indicate that the VAMs due to heading variations are predominant, similarly to what was observed for the bicycle.

The significant number of VAMs due to heading variations that we observed raised the following questions: does the $\Delta_h = 4°$ threshold represent the most proper choice for the examined VRUs? Or should a more carefully selected value

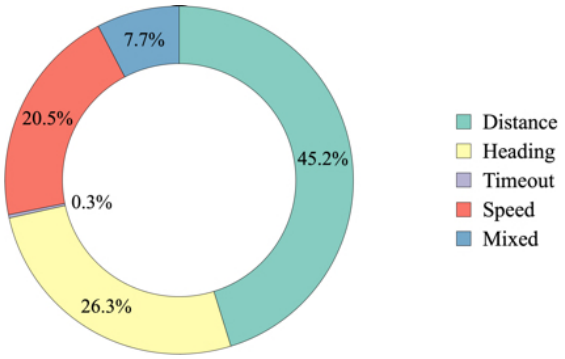

(a) Triggers distribution.

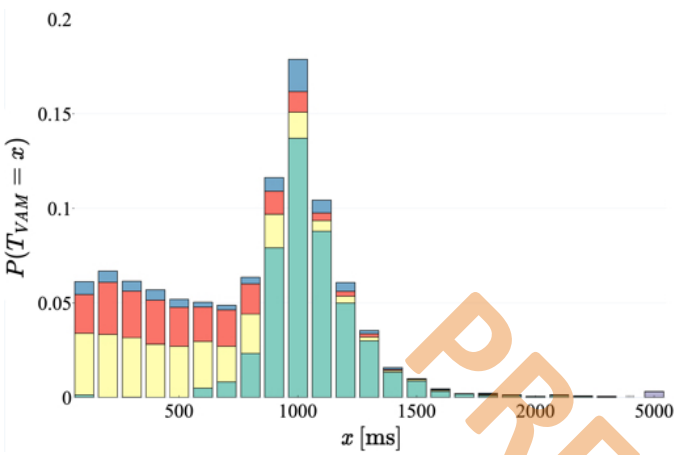

(b) PMF.

Fig. 7. Bicycle: VAM triggers and T_{VAM} PMF for $\Delta_h = 10°$.

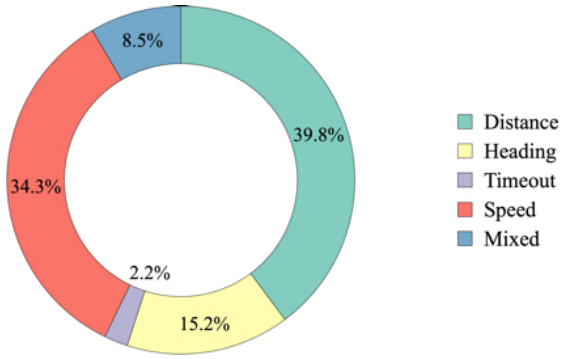

(a) Triggers distribution.

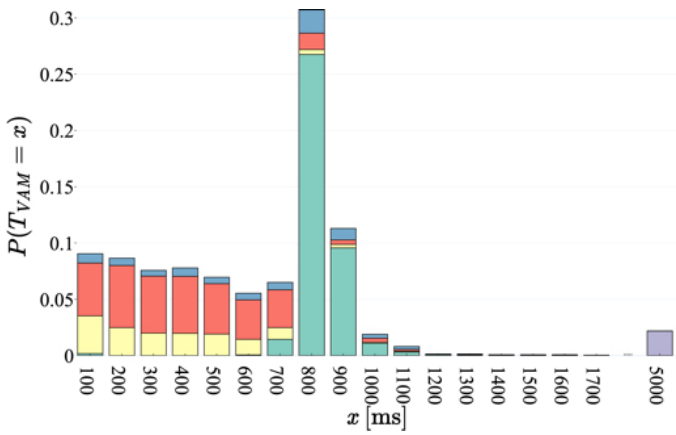

(b) PMF.

Fig. 8. E-scooter: VAM triggers and T_{VAM} PMF for $\Delta_h = 10°$.

be employed?

To help identify the correct answers, the next set of figures considers an exemplary portion of the bicycle rides, and plots on the map the GNSS coordinates where VAMs generated by heading variations were broadcasted. Fig. 6(a) refers to $\Delta_h = 4°$ and shows that a remarkable fraction of such VAMs is transmitted under non-relevant circumstances, i.e., on a straight road segment. These VAMs are useless to other road traffic participants. Figs. 6(b) and (c) correspond to a progressively increased value of Δ_h, $\Delta_h = 7°$ and $10°$, respectively. The figures show that an increase of the Δ_h threshold reduces the number of heading-generated VAMs, without diminishing their effectiveness for Δ_h up to $10°$. In this case, Fig. 6(c) indicates that heading variations generate new VAMs only when the VRU performs a relevant steering movement.

Figs. 7(a)-(b) analyze the VAMs generated when $\Delta_h = 10°$, the values of Δ_d and Δ_s being unmodified. Fig. 7(a) quantifies the impact of the $\Delta_h = 10°$ setting on the percentage of each trigger type. With respect to Fig. 4(a), the percentage of VAMs triggered by heading variations decreases from 74% to 26.3%, whereas the percentage of VAMs triggered by speed and distance increases from 6.8% to 20.5%, and from 11% to 45.2%, respectively. Fig. 7(b) completes the analysis, reporting the PMF of the T_{VAM}, where a significant reduction in heading-generated VAMs is observed, with respect to Fig. 4(a). As a result, the contribution of speed and distance triggers is more evident, and the PMF profile is shifted towards larger T_{VAM} values.

The impact of a larger Δ_h threshold on the e-scooter VAMs is also analyzed in Figs. 8(a)-(b). Fig. 8(a) quantifies the impact of the $\Delta_h = 10°$ setting on the percentages of VAMs due to each trigger type; the reduction of heading-generated VAMs is evident from the comparison with Fig. 5(a). Fig. 8(b) reports the PMF of T_{VAM}, revealing that the probabilities associated with the most populated T_{VAM} bins (at 800 and 900 ms) are markedly higher.

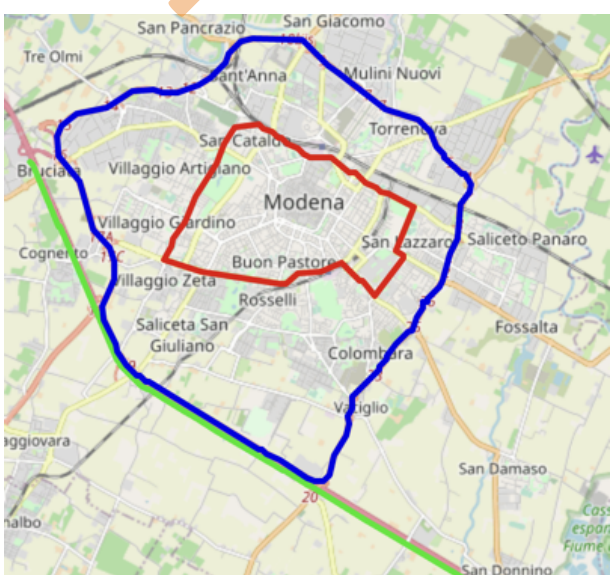

Fig. 9. The examined scenarios.

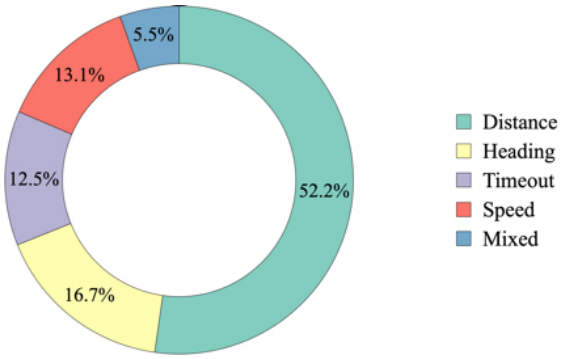

(a) Triggers distribution.

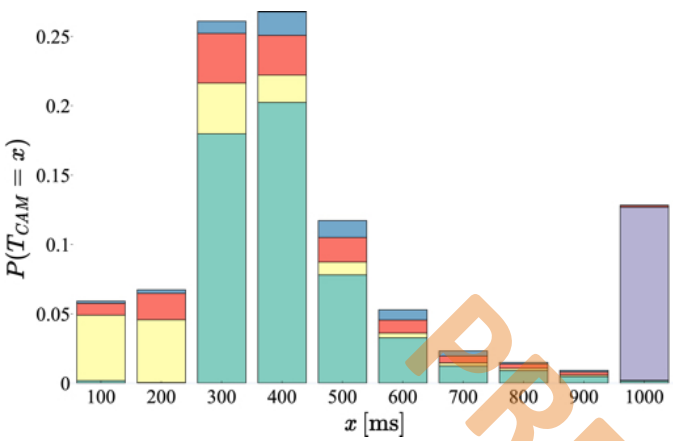

(b) PMF.

Fig. 10. Car: CAM triggers and T_{CAM} PMF, *urban* scenario.

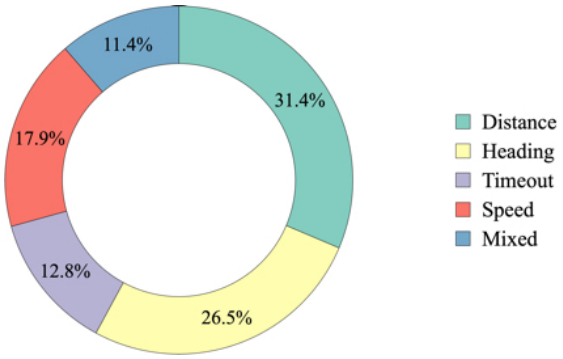

(a) Triggers distribution.

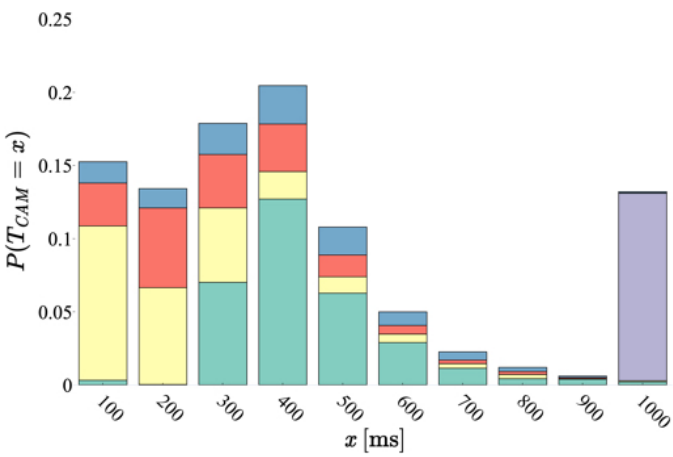

(b) PMF.

Fig. 11. Motorcycle: CAM triggers and T_{CAM} PMF, *urban* scenario.

C. Vehicle and Motorcycle CAMs

The test results about the generation times of CAMs by cars and motorbikes are reported next, for $\Delta_d = 4$ m, $\Delta_h = 4°$, and $\Delta_s = 0.5$ m/s. Although motorcycles are classified as VRUs, note that they transmit CAMs, not VAMs [28]. For cars, the measurements were performed in three different settings: an urban environment, a suburban area, and a highway. For motorbikes, the urban scenario only was examined. Cars and motorbikes traveled among other vehicles, experiencing normal daytime traffic conditions. The macroscopic description of the propagation environments that vehicles experienced is the following: (i) the urban route mainly consists of large avenues surrounded by trees and residential buildings; (ii) the suburban route is made of road portions that run close to constructions, while other segments run through open areas; (iii) the highway crosses a mixed area, with cultivated fields and industrial plants.

The car repeatedly traveled along the urban path depicted in red in Fig. 9, where varied traffic conditions were encountered, traffic lights forced vehicles to stop and roundabouts slowed them down. Fig. 10(a) reports the percentage of the different triggering conditions and Fig. 10(b) the PMF of T_{CAM}, the time interval between two consecutive CAMs. Fig. 10(a) indicates that distance variations greater than 4 m are the main cause behind CAM generation in this setting; they trigger more than half of the recorded messages. In order of decreasing influence, distance is followed by heading, speed, timeout, and mixed triggers. Except for the latter, the figure indicates that the other conditions have a comparable effect. Compared to the VAMs generated by bicycles and e-scooters with $\Delta_h = 4°$, the heading variation weighs much less. However, as visible from Fig. 10(b), it still accounts for most triggering conditions when $T_{CAM} = 100$ ms and 200 ms. Moreover, CAMs due to distance variations greater than 4 m are generated with a lower T_{CAM}. This is due to the higher speeds of the vehicle: we recorded 29.7 km/h for the average and 71.9 km/h for the maximum. The other relevant difference concerning VAMs pertains to the timeouts, nearly absent in all results presented in Section IV-B. Here, they account for 12.5% of the triggering conditions, corresponding to a T_{CAM} of 1000 ms.

Regarding the same urban scenario, Fig. 11 reports the percentage of the triggering conditions and the PMF of T_{CAM} for a two-wheel motorbike. Comparing the percentages of the motorbike triggering conditions in Fig. 11(a) with those of the car in Fig. 10(a), it is concluded that they are more diversified. Distance variations account for approximately 30% of the total, heading variations are significantly more frequent, and the occurrences of the speed and mixed conditions are increased. Only the timeout percentage stays approximately the same. The most significant phenomenon is that CAMs generated by heading variations become more frequent. Indeed, a motorbike follows a more irregular trajectory than a car, due to its smaller size and agility in slipping through traffic. Fig. 10(b) also reveals that heading variations are mainly responsible for generating CAMs whose T_{CAM} is lower than 300 ms; above

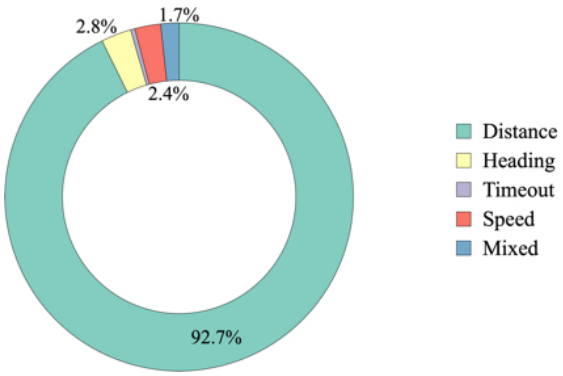

(a) Triggers distribution.

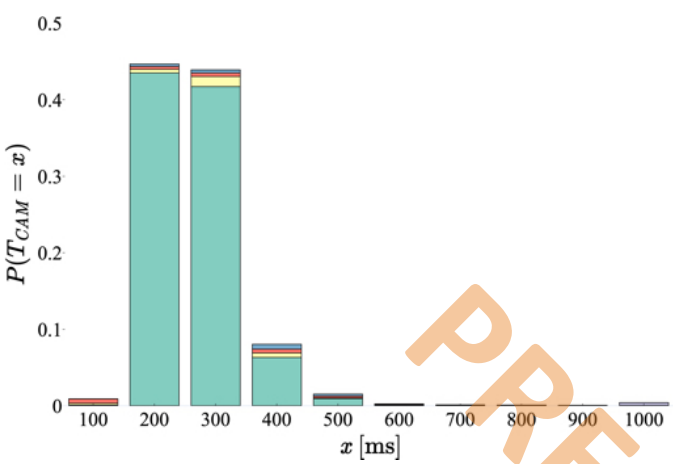

(b) PMF.

Fig. 12. Car: CAM triggers and T_{CAM} PMF, *suburban* scenario.

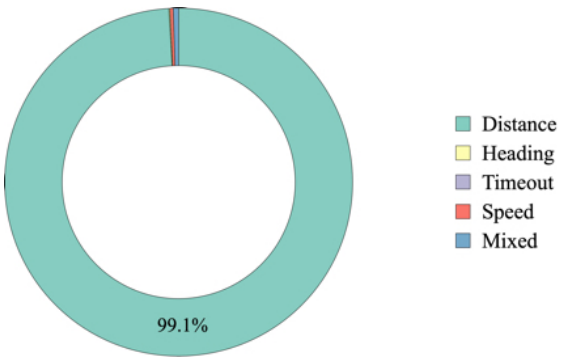

(a) Triggers distribution.

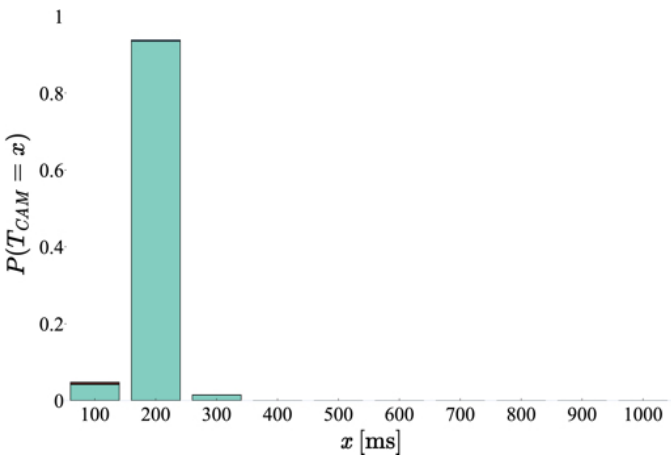

(b) PMF.

Fig. 13. Car: CAM triggers and T_{CAM} PMF, *highway* scenario.

this value, CAMs caused by distance variations, i.e., higher speeds, prevail.

The measurement campaign was completed by tests performed having the cars also traveling on suburban roads and on a highway. In the first case, the route followed by the car is reported in blue in Fig. 9, and refers to the freeway belt surrounding Modena. The corresponding percentages of triggering conditions and the PMF of T_{CAM} are provided in Figs. 12(a) and 12(b), respectively. Here, distance accounts for the vast majority of the generated CAMs. Timeouts are negligible, while heading, velocity, and mixed altogether cause $\sim 7\%$ of the CAMs. The vast majority of the CAMs is triggered in the time interval $[200, 300]$ ms, which corresponds to the $[48, 144]$ km/h range of speed values [23].

As regards the highway, the drive route is evidenced in green in Fig. 9. Fig. 13(a) reports the percentages of the triggering conditions, and Fig. 13(b) the PMF of T_{CAM}. Distance variations cause more than 99% of the CAMs. Due to the higher speeds, the vast majority of CAMs are triggered because of distance with a time interval between two subsequent messages of 200 ms. This is because $T_{CAM} = 300$ ms corresponds to velocities in the $[48, 72)$ km/h range, $T_{CAM} = 200$ ms to velocities in the $[72, 144)$ km/h range, and $T_{CAM} = 100$ ms to speeds higher than 144 km/h [23]. The car speed exhibited an average of 116.7 km/h and a maximum of 148.5 km/h. Because of varying traffic conditions, there were cases in which vehicles were traveling below 72 km/h, which in turn account for $T_{CAM} = 300$ ms. Overall, the PMF resulted nearly unimodal. Although some of the results referring to vehicles could be drawn by simulation, we observe that a simulator cannot perfectly replicate the vehicle dynamics. This is particularly true in environments where the driver's behavior heavily depends on the road topology and the dynamics of other road users. To conclude, only the measurement campaign offers a realistic picture of what to expect.

The number of collected messages, the test duration, and the traveled distance are summarized in Tables II and III for all the examined road users.

D. Collected and Simulated CAMs Comparison

Although consolidated models exist to simulate road mobility, empirical measurements are nevertheless necessary; they are key in validating numerical approaches and identifying circumstances where simulation falls short. To corroborate the last statement and demonstrate the usefulness of our field campaign, we employed the vehicular micromobility simulator SUMO [42] to generate a synthetic dataset of CAM traces in the same urban, suburban, and highway routes as in the experimental tests. We imported the street layout of the city of Modena in SUMO using Open Street Map [43], and populated the road network with three different vehicular densities, namely: low, medium, and high. The low density case repre-

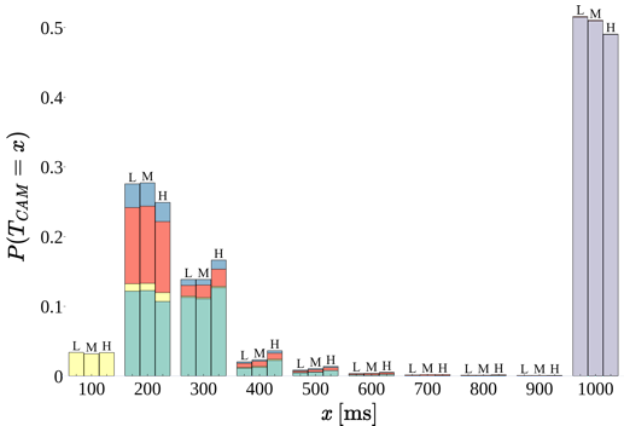

(a) *Urban* scenario.

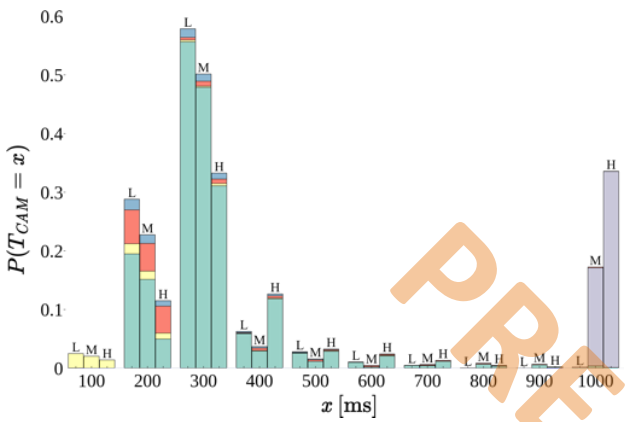

(b) *Suburban* scenario.

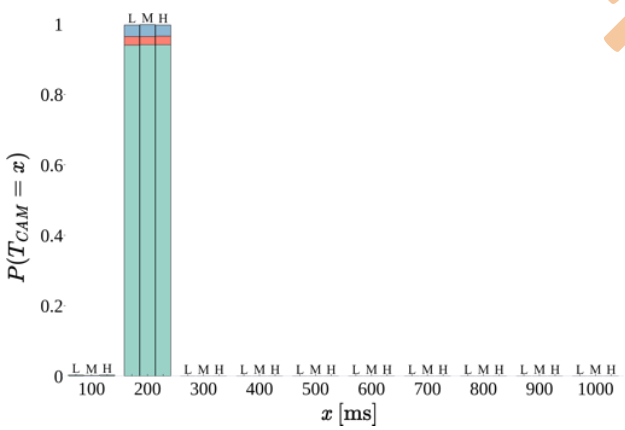

(c) *Highway* scenario.

Fig. 14. Synthetic dataset: T_{CAM} PMF in the urban, suburban, and highway scenario under different traffic conditions.

(a) Tx bicycle: setup.

(b) Tx and Rx car: rooftop antennas.

(c) Rx car: in-vehicle setup.

Fig. 15. LTE-V2X PDR: employed equipment.

sents an uncongested road network; the high vehicular density reflects peak hour traffic conditions.

After running a sufficiently large number of simulations, we obtained more than 5×10^5 synthetic CAMs for each scenario and analyzed the PMF of the time between consecutive messages, T_{CAM}. Fig. 14 reports the PMFs obtained in the urban, suburban, and highway settings considering the low, medium, and high vehicular densities, denoted by L, M, and H, respectively. Fig. 14(a) refers to the urban scenario and reveals non-negligible discrepancies with respect to the experimental outcomes of Fig. 10(b), no matter what vehicular density is examined. Most notably, in the simulation, the probability of generating a CAM due to the timeout condition, i.e., $P[T_{CAM} = 1000 \text{ ms}]$, is 0.5 and represents the most significant contribution. This happens since SUMO wrongly mimics the behavior of cars at intersections and roundabouts. In SUMO, vehicles cross an intersection or enter a roundabout

only when their maneuvers do not force other vehicles to slow down. This behavior is responsible for long queues of vehicles even in the low density setting, causing timeout triggers which do not occur in reality. When the suburban scenario is examined, SUMO exhibits a similar misbehavior in correspondence of acceleration ramps. For this reason, the T_{CAM} PMF reported in Fig. 14(b) is characterized by a significantly larger probability of triggering the timeout condition with respect to its experimental counterpart in Fig. 12(b). In Fig. 14(b), note that $P[T_{CAM} = 1000 \text{ ms}]$ becomes larger as the vehicular density increases. The highway scenario is the only setting where simulative and experimental results match, as the comparison between Figs. 13(b) and 14(c) indicate. To conclude, simulations do not always correctly replicate the vehicles' dynamics, and measurement campaigns are necessary to understand what to expect in reality.

E. LTE-V2X Packet Delivery Ratio

We next determined the PDR achieved for two distinct cases: (i) a bicycle broadcasting VAMs and a car receiving them; (ii) a car broadcasting CAMs, while a second car was driving behind and acting as the receiver. Note that message losses were exclusively due to varying propagation conditions, given no additional traffic was injected on the radio channel to cause congestion and harm the VAM and CAM dissemination.

The cars and the bicycle were equipped with the LTE-V2X evaluation boards. Fig. 15 displays the equipment deployed in the two cases. When positioned on the bicycle, the antennas were directly connected to the board and their height was 0.80 m; on the car rooftop, the antennas' height was 1.45 m. Three evaluation boards were utilized for this set of measurements. The transmitting board was placed in the front vehicle or in the bicycle basket, generating the awareness messages. Two boards were placed on the receiving vehicle, one acted as the receiver, and another recorded the GNSS outputs every 50 ms. This allowed for the continuous tracking of the receiving car position, which would otherwise occur only at the successful reception of a message. By doing so, we were able to reliably compute the PDR as a function of the distance between the two road occupants. All other relevant settings, such as transmit power, MCS, code rate, and receiver sensitivity were those listed in Subsection IV-A.

When considering VAMs transmitted from the bicycle, Fig. 16 portrays the PDR as a function of D, the distance between the transmitting bicycle and the receiving car, in the urban environment. The black scatter plot shows the PDR mean values; the box plots, i.e., the vertical, light blue lines, indicate the 95% confidence interval of the measurements. The figure shows that the reliability range, i.e., the distance at which the PDR falls below 0.9 is 125 m, and that the communication range, i.e., the distance beyond which the PDR goes to zero, is 600 m.

Figs. 17(a), 17(b), and 17(c) portray the PDR attained by CAM dissemination as a function of D, the distance between the transmitting and the receiving cars, in the urban, suburban and highway scenarios, respectively. In the urban setting, the PDR curve is consistently higher than in the case of

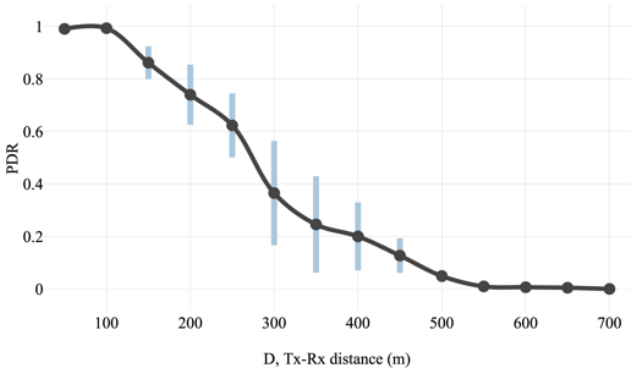

Fig. 16. Bicycle-to-Vehicle communications: Packet Delivery Ratio.

VAM transmission; this is explained by a more favorable placement of the antennas on the car, which benefits from a higher elevation from the ground than in the case of the bicycle. The reliability range is 250 m and the communication range is 700 m. In this setting, the communication range is limited by the presence of buildings that block the Line-Of-Sight (LOS) path. The former value is far lower than the one obtained in Non-Line-Of-Sight (NLOS) condition in [24], where the authors report 875 m at an intersection and 425 m in the case of a strong obstruction. In the suburban setting, packets were delivered over an extended distance, as very few buildings could disrupt the communications. Yet, many vehicles, including trucks, populate the two-lane road of the drive route. Fig. 17(b) accordingly shows that the reliability range is 250 m, whereas the communication range extends to 1000 m. Last, Fig. 17(c) refers to the highway scenario. On the highway, cars were able to communicate more reliably and over longer distances because there were seldom any obstacles between them. In this case, the reliability range is 700 m; moreover, the communication range is slightly lower than 2000 m. Comparing these outcomes with the findings in [24] that refer to LOS conditions, we observe that in [24] the reliability range was measured at nearly 1200 m, i.e., a much larger value. There are fewer discrepancies when our results are compared with those in [22], where the PDR crosses the 0.9 threshold at $D = 500$ m.

In parallel, we monitored the delay incurred by packets and verified that it respected the packet delay budget, set to 50 ms. This is a direct consequence of the nearly deterministic channel access mechanism that LTE-V2X adopts.

F. Discussion

1) VAM and CAM generation times: The tests have revealed that the Δ_h value bikes and e-scooters inherit by the vehicular setting is excessively low. It causes a significant number of VAMs to be generated under non-relevant circumstances, providing neighboring road users no useful clues about the VRU dynamics and wasting precious radio resources. Properly setting Δ_h to the slightly larger value of 10° solves the problem, with no loss of meaningful information about the VRU status. The significant increase in the average T_{VAM} that this modification achieves can be

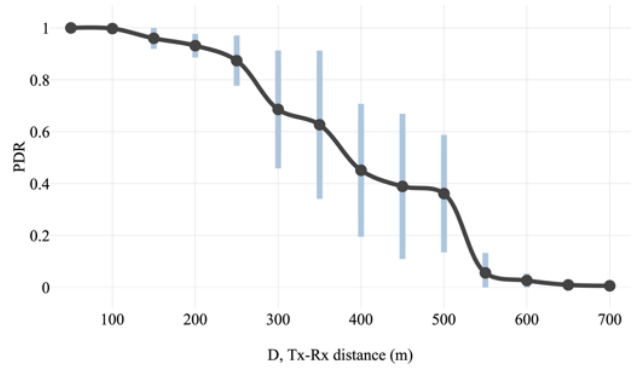

(a) *Urban* scenario.

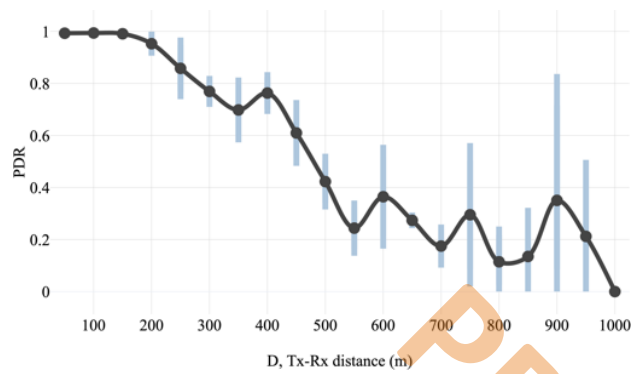

(b) *Suburban* scenario.

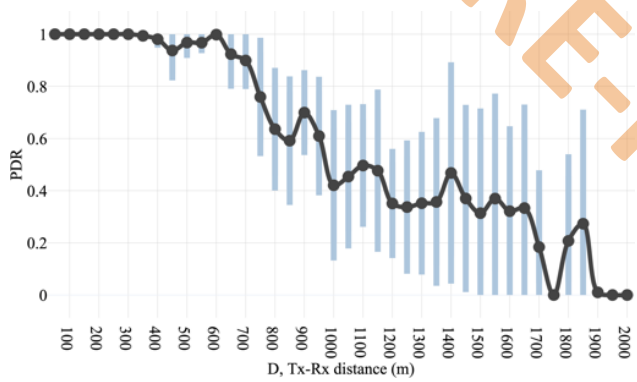

(c) *Highway* scenario.

Fig. 17. V2V communications: Packet Delivery Ratio.

appreciated by comparing the values of Table IV. The benefit is relevant, especially in the light of an increase in the number of connected VRUs, and if the operation of each VRU will be subject to spectrum usage constraints [28].

The field tests performed with the motorbike indicate that the number of distance and heading triggers is comparable for CAMs generated by this category of VRUs. It is furthermore observed that motorbikes generate more varied CAM traffic than cars. In the urban setting, the average T_{CAM} is 270 ms, far lower than for cars, whose value is 460 ms, and it reflects the typical hasty nature of motorbike drivers. Table IV provides an overall numerical picture of our measured T_{VAM} and T_{CAM} values.

The tests performed with cars show that: (i) distance variations are the main CAM triggering cause, followed by speed variations; (ii) the T_{CAM} PMF is strongly multimodal in the urban scenario and reduces to being almost unimodal in the highway scenario. The obtained PMFs depart from those obtained by simulation, highlighting the limits of this approach and the value of field tests. Moreover, the highway PMF largely differs from the results reported in previous studies [23]. We believe that the discrepancy is due to the limited size of the data set employed by the authors of the latter study.

2) LTE-V2X PDR: We assessed the PDR of the LTE-V2X technology for direct VRU-to-vehicle and V2V communications, clearly identifying the challenges faced by the delivery of awareness messages. No tests were ever presented in the literature for VRU communications, and our experiments highlighted that in the urban setting, the transmission of VAMs can count on reduced reliability and communication range with respect to CAMs.

For V2V communications, we offered a complete and realistic picture referring to distinct settings and found more pessimistic range values than the authors of [24]. In this respect, we would like to stress that we considered actual environments, not a test track. Our tests indicate that the CAM reliability and communication range significantly depend on the examined context, and increase when LOS conditions are more frequently encountered.

It is worth highlighting that these results have been obtained considering a single transmitter-receiver pair, i.e., without interfering vehicles. Further limitations in the reliability and communication range might be encountered if we consider a larger number of simultaneously transmitting vehicles and the impact of co-channel interference, i.e., packet collisions.

As anticipated in the Introduction, all measurement data referring to VAMs, CAMs, and PDR values are freely accessible on GitHub [13].

3) Impact on road safety: Although this work mainly concentrates on the analysis of the inter-arrival time between awareness messages and on their generation causes, the obtained results provide some preliminary insights on the impact that CAMs and VAMs dissemination will have on road safety. To this end, we leverage the average T_{VAM} and T_{CAM} values of Table IV, together with the average speed measured during our experiments (reported in Table V), to calculate the average update distance. This is determined as the product between the average inter-arrival time and the average speed, and corresponds to the average distance traveled by a road user (vehicle or VRU) before broadcasting an awareness message. Therefore, the average update distance indicates how frequently vehicles and VRUs announce their presence

TABLE IV
AVERAGE T_{VAM} AND T_{CAM} VALUES.

Vehicle type	Urban	Suburban	Highway
Bicycle - $\Delta_h = 4°$	435 ms	-	-
Bicycle - $\Delta_h = 10°$	831 ms	-	-
E-scooter - $\Delta_h = 4°$	474 ms	-	-
E-scooter - $\Delta_h = 10°$	702 ms	-	-
Motorbike	270 ms	-	-
Car	460 ms	256 ms	197 ms

TABLE V
AVERAGE SPEED VALUES.

Vehicle type	Urban	Suburban	Highway
Bicycle	12.9 km/h	-	-
E-scooter	14 km/h	-	-
Motorbike	35.2 km/h	-	-
Car	29.7 km/h	74.5 km/h	116.7 km/h

TABLE VI
AVERAGE UPDATE DISTANCE VALUES.

Vehicle type	Urban	Suburban	Highway
Bicycle - $\Delta_h = 4°$	1.56 m	-	-
Bicycle - $\Delta_h = 10°$	2.97 m	-	-
E-scooter - $\Delta_h = 4°$	1.84 m	-	-
E-scooter - $\Delta_h = 10°$	2.73 m	-	-
Motorbike	2.64 m	-	-
Car	3.79 m	5.29 m	6.39 m

in the spatial domain, allowing neighboring road users and the roadside infrastructure to enforce dedicated road safety policies upon the reception of the transmitted messages.

The first column of Table VI, reporting the average update distance values, shows that bicycles and e-scooters generate a new awareness message every 1.56 m and 1.84 m when the default heading threshold ($\Delta_h = 4°$) is considered. When the heading threshold is increased to 10°, and the number of non-relevant VAMs triggered by heading variations is reduced, the average T_{VAM} increases (see Table IV). As a consequence, also the average update distance increases, growing from 1.56 m to 2.97 m in the bicycle case, and from 1.84 m to 2.73 m for the e-scooter. Despite such an increase, note that these values are in line with those obtained for the car and the motorbike in the urban setting, thus demonstrating that the heading threshold adjustment proposed in this work does not deteriorate the effectiveness of VAM dissemination. Due to the higher vehicle's speed, the average update distance of vehicles in the suburban and highway settings increases to 5.29 m and 6.39 m, respectively.

V. CONCLUSIONS AND FUTURE WORK

This work has presented the results of a measurement campaign whose first aim has been to investigate the temporal dynamics of awareness messages and their generation causes. VAMs and CAMs were gathered through numerous field tests performed in urban, suburban, and highway settings. The analysis of the collected data has revealed the impact of the various triggering conditions of both messages in the distinct environments where road occupants travel.

Concerning the urban scenario, the study has highlighted the unique characteristics of VAMs issued by bicycles and e-scooters, and has pointed to an amendment of their generation rule that diminishes their frequency without any relevant information loss. This turns out especially relevant if many VRUs are equipped with a transmitting device and the risk of creating congestion on the radio channel becomes tangible. In the same setting, the paper has shown that the VRU category represented by motorbikes exhibits a distinctive PMF of the time between consecutive CAMs and that the conditions that trigger its CAM broadcasting are peculiar as well. As regards cars, distance variations are always the main reason behind CAM generation; their CAMs become more frequent and the PMF of T_{CAM} accordingly shifts toward lower values and becomes more peaked when moving from the busy traffic conditions of the urban environment to the smoother driving scene of the highway.

This work has also evaluated the PDR experienced by the LTE-V2X technology in vehicle-to-vehicle and, for the first time, bicycle-to-vehicle communications. The actual communication range and the reliability range that VAM and CAM broadcasting can accomplish in the urban, suburban, and highway setting were identified. Furthermore, all data collected during the field tests have been openly released, to ease the research of the community working on road safety solutions.

To conclude, several research paths are suggested by the measurement campaign, the most immediate being the proposal of alternative algorithms for the generation of VAMs by different categories of VRUs. Namely, bikes and e-scooters may still adhere to ETSI specifications to broadcast VAMs, although with adaptive thresholds, or may generate VAMs with adaptive frequencies, e.g., dependent on their speed. At the same time, the impact of CAM and VAM dissemination on road safety should be carefully assessed. To this end, the development of novel simulation tools and the introduction of safety-oriented performance metrics is of paramount importance. On the other hand, it is our belief that pedestrians will not necessarily be connected: rather, it will be up to connected vehicles to sense their presence and share this knowledge with other road occupants through a smart road infrastructure, exchanging richer and more structured messages than VAMs and CAMs, e.g., cooperative perception messages.

REFERENCES

[1] IEEE Standard for Information technology - Local and metropolitan area networks - Specific requirements - Part 11: Wireless LAN Medium Access Control (MAC) and Physical Layer (PHY) Specifications Amendment 6: Wireless Access in Vehicular Environments, https://standards.ieee.org/ieee/802.11p/3953/.

[2] J.B. Kenney, "Dedicated Short-Range Communications (DSRC) Standards in the United States," in *Proc. of the IEEE*, vol. 99, no. 7, pp. 1162-1182, July 2011.

[3] European Telecommunications Standards Institute (ETSI), "ITS-G5 Access layer specification for Intelligent Transport Systems operating in the 5 GHz frequency band," EN 302 663 V1.3.1, October 2019.

[4] R. Molina-Masegosa and J. Gozalvez, "LTE-V for Sidelink 5G V2X Vehicular Communications: A New 5G Technology for Short-Range Vehicle-to-Everything Communications," in *IEEE Veh. Tech. Mag.*, vol. 12, no. 4, pp. 30-39, Dec. 2017.

[5] V. Mannoni, V. Berg, S. Sesia and E. Perraud, "A Comparison of the V2X Communication Systems: ITS-G5 and C-V2X," *2019 IEEE 89th Vehicular Technology Conference (VTC2019-Spring)*, 2019, pp. 1-5.

[6] M. Gonzalez-Martín, M. Sepulcre, R. Molina-Masegosa and J. Gozalvez, "Analytical Models of the Performance of C-V2X Mode 4 Vehicular Communications," in *IEEE Trans. on Veh. Tech.*, vol. 68, no. 2, pp. 1155-1166, Feb. 2019.

[7] R. Molina-Masegosa, J. Gozalvez and M. Sepulcre, "Comparison of IEEE 802.11p and LTE-V2X: An Evaluation With Periodic and Aperiodic Messages of Constant and Variable Size," in *IEEE Access*, vol. 8, pp. 121526-121548, 2020.

[8] K. Z. Ghafoor, M. Guizani, L. Kong, H. S. Maghdid and K. F. Jasim, "Enabling Efficient Coexistence of DSRC and C-V2X in Vehicular Networks," in *IEEE Wireless Communications*, vol. 27, no. 2, pp. 134-140, April 2020.

[9] European Telecommunications Standards Institute (ETSI), "Intelligent Transport Systems (ITS); Vehicular Communications; Basic Set of Applications; Specification of Cooperative Awareness Basic Service," EN 302 637-2 V1.4.1, April 2019.

[10] European Telecommunications Standards Institute (ETSI), "Intelligent Transport Systems (ITS); Vulnerable Road Users (VRU) awareness; Part 3: Specification of VRU awareness basic service; Release 2," TS 103 300-3 V2.1.1, November 2020.

[11] 5G Automotive Association (5GAA), "Vulnerable Road User Protection," White Paper, August 2020. [Online]. Available: https://5gaa.org/news/vulnerable-road-user-protection/.

[12] CAR 2 CAR Communication Consortium, "Study of Vulnerable Road User awareness," White Paper, February 2021.

[13] Open source repository with the presented CAMs and VAMs dataset: https://github.com/LLusvarghi/CAM-VAM-dataset.

[14] K. Saleh, M. Hossny and S. Nahavandi, "Contextual Recurrent Predictive Model for Long-Term Intent Prediction of Vulnerable Road Users," in *IEEE Trans. on Intell. Transp. Syst.*, vol. 21, no. 8, pp. 3398-3408, Aug. 2020.

[15] M. Goldhammer, S. Kohler, S. Zernetsch, K. Doll, B. Sick and K. Dietmayer, "Intentions of Vulnerable Road Users-Detection and Forecasting by Means of Machine Learning," in *IEEE Trans. on Intell. Transp. Syst.*, vol. 21, no. 7, pp. 3035-3045, July 2020.

[16] V. R. S. Banjade, S. C. Jha, K. Sivanesan, L. Gomes Baltar, S. A. Sehra and S. J. Tan, "Vulnerable Road Users Safety in Infrastructure Assisted Intelligent Transportation System," *2021 IEEE Int. Smart Cities Conf. (ISC2)*, 2021, pp. 1-7.

[17] S. Lobo, A. Festag and C. Facchi, "Enhancing the Safety of Vulnerable Road Users: Messaging Protocols for V2X Communication," 2022 IEEE 96th Vehicular Technology Conference (VTC2022-Fall), London, United Kingdom, 2022, pp. 1-7.

[18] M. Shan, K. Narula, Y. F. Wong, S. Worrall, M. Khan, P. Alexander and E. Nebot, "Demonstration of Cooperative Perception: Safety and Robustness in Connected and Automated Vehicle Operations," in *MDPI Sensors*, vol. 21, no. 1, 2021.

[19] Deliverable D5.2, the 5GCAR Demonstrations Version [Online]. Available://5gcar.eu/

[20] M. Boban and P. M. d'Orey, "Exploring the Practical Limits of Cooperative Awareness in Vehicular Communications," in *IEEE Trans. on Veh. Technol.*, vol. 65, no. 6, pp. 3904-3916, June 2016.

[21] E. Moradi-Pari, D. Tian, M. Bahramgiri, S. Rajab and S. Bai, "DSRC Versus LTE-V2X: Empirical Performance Analysis of Direct Vehicular Communication Technologies," in *IEEE Trans. on Intell. Trans. Syst.*, 2023.

[22] V. Maglogiannis, D. Naudts, S. Hadiwardoyo, D. van den Akker, J. Marquez-Barja and I. Moerman, "Experimental V2X Evaluation for C-V2X and ITS-G5 Technologies in a Real-Life Highway Environment," in *IEEE Trans. on Netw. and Service Manage.*, November 2021.

[23] CAR 2 CAR Communication Consortium, "Survey on ITS-G5 CAM statistics," TR2052, V1.0.1, Dec. 2018.

[24] 5G Automotive Association (5GAA), "V2X Functional and Performance Test Report; Test Procedures and Results," 5GAA P-190033, April 2019.

[25] G. Twardokus and H. Rahbari, "Towards Protecting 5G Sidelink Scheduling in C-V2X Against Intelligent DoS Attacks," in *IEEE Trans. on Wireless Commun.*, 2023.

[26] L. Lusvarghi and M. L. Merani, "On the Coexistence of Aperiodic and Periodic Traffic in Cellular Vehicle-to-Everything," in *IEEE Access*, vol. 8, pp. 207076-207088, 2020.

[27] L. Lusvarghi and M. L. Merani, "Machine Learning for Disseminating Cooperative Awareness Messages in Cellular V2V Communications," in *IEEE Trans. on Veh. Technol.*, vol. 71, no. 7, pp. 7890-7903, July 2022.

[28] European Telecommunications Standards Institute (ETSI), "Intelligent Transport Systems (ITS); Vulnerable Road Users (VRU) awareness; Part 1: Use Cases definition; Release 2," ETSI TR 103 300-1 V2.1.1, September 2019.

[29] European Telecommunications Standards Institute (ETSI), "Intelligent Transport System (ITS); Vulnerable Road Users (VRU) awareness; Part 2: Functional Architecture and Requirements definition; Release 2," ETSI TS 103 300-2 V2.1.1, May 2020.

[30] Society of Automotive Engineers (SAE), "Vulnerable Road User Safety Message Minimum Performance Requirements," SAE J 2945/9, March 2017.

[31] I. Rashdan, M. Schmidhammer, F. de Ponte Mueller and S. Sand, "Performance Evaluation of Vehicle-to-Vehicle Communication for Cooperative Collision Avoidance at Urban Intersections," *2017 IEEE 86th Veh. Tech. Conf. (VTC-Fall)*, 2017, pp. 1-5.

[32] M. Elhenawy, A. Bond and A. Rakotonirainy, "C-ITS Safety Evaluation Methodology based on Cooperative Awareness Messages," *2018 21st International Conference on Intell. Transp. Syst. (ITSC)*, 2018, pp. 2471-2477.

[33] L. Gibellini and M. L. Merani, "Out-of-Coverage Multi-Hop Road Safety Message Distribution via LTE-A Cellular V2V (C-V2V)," *2018 IEEE 88th Veh. Tech. Conf. (VTC-Fall)*, 2018, pp. 1-6.

[34] R. Molina-Masegosa, M. Sepulcre, J. Gozalvez, F. Berens and V. Martinez, "Empirical Models for the Realistic Generation of Cooperative Awareness Messages in Vehicular Networks," in *IEEE Trans. on Veh. Technol.*, vol. 69, no. 5, pp. 5713-5717, May 2020.

[35] J. Aznar-Poveda, E. Egea-López and A. García-Sánchez, "Cooperative Awareness Message Dissemination in EN 302 637-2: an Adaptation for Winding Roads," *2020 IEEE 91st Veh. Technol. Conf. (VTC2020-Spring)*, 2020, pp. 1-5.

[36] M. Sepulcre, J. Gozalvez, G. Thandavarayan, B. Coll-Perales, J. Schindler and M. Rondinone, "On the Potential of V2X Message Compression for Vehicular Networks," in *IEEE Access*, vol. 8, pp. 214254-214268, 2020.

[37] M. H. C. Garcia et al., "A Tutorial on 5G NR V2X Communications," in *IEEE Communications Surveys & Tutorials*, vol. 23, no. 3, pp. 1972-2026, 2021.

[38] Quectel AG15 Module, Product Specifications. [Online]. Available: https://www.quectel.com/product/c-v2x-ag15.

[39] European Telecommunications Standards Institute (ETSI), "Intelligent Transport Systems (ITS); Radiocommunications equipment operating in the 5855 MHz to 5925 MHz frequency band; Harmonised Standard covering the essential requirements of article 3.2 of Directive 2014/53/EU," ETSI EN 302 571 V2.1.1, February 2017.

[40] W. Anwar, N. Franchi and G. Fettweis, "Physical Layer Evaluation of V2X Communications Technologies: 5G NR-V2X, LTE-V2X, IEEE 802.11bd, and IEEE 802.11p," *2019 IEEE 90th Veh. Technol. Conf. (VTC2019-Fall)*, 2019, pp. 1-7.

[41] A. Bazzi, G. Cecchini, M. Menarini, B. M. Masini and A. Zanella, "Survey and Perspectives of Vehicular Wi-Fi versus Sidelink Cellular-V2X in the 5G Era," in *MDPI Future Internet*, vol. 11, no. 6, 2019.

[42] P. A. Lopez et al., "Microscopic traffic simulation using SUMO," in Proc. 21st Int. Conf. Intell. Transp. Syst. (ITSC), Maui, HI, USA, 2018, pp. 2575–2582.

[43] OpenStreetMap contributors, "Planet dump retrieved from https://planet.osm.org," Accessed: Jan. 10, 2023. [Online]. Available: https://www.openstreetmap.org/.